



Highly dispersed Pt nanoparticle catalyst prepared by atomic layer deposition

Jianhua Li^a, Xinhua Liang^a, David M. King^a, Ying-Bing Jiang^b, Alan W. Weimer^{a,*}

^a Department of Chemical and Biological Engineering, University of Colorado, Boulder, CO 80309-0424, USA

^b Department of Earth and Planetary Sciences, University of New Mexico, Albuquerque, NM 87131, USA

ARTICLE INFO

Article history:

Received 28 October 2009

Received in revised form 23 March 2010

Accepted 8 April 2010

Available online 14 April 2010

Keywords:

Silica gel

Mesoporous

Catalyst

Platinum

Atomic layer deposition

ABSTRACT

Nanoparticulate platinum has been well dispersed onto large quantities of micron-sized mesoporous silica gel using atomic layer deposition in a fluidized bed reactor (i.e. ALD-FBR). Transmission electron microscopy (TEM) cross-sectional investigations showed that the Pt nanoparticles were homogeneously distributed throughout primary 30–75 μm silica gel particles, including the inner surfaces comprising 5–7 nm pores. The Pt catalyst loading level was tightly controlled by the number of coating cycles. An extremely low Pt loading with 3.1×10^{-6} mg Pt/cm² (0.10 atom/nm²), 4.8×10^{-6} mg Pt/cm² (0.15 atom/nm²) and 2.9×10^{-5} mg Pt/cm² (0.91 atom/nm²) was prepared with 3, 5 and 10 coating cycles, respectively. The average Pt particle size is approximately 1.2 nm for 3 cycles. For 5 and 10 coating cycles, the Pt particle size is measured to be 1.9 nm and 2.3 nm, respectively. The sample with a 3.1×10^{-6} mg Pt/cm² loading exhibits the highest metal dispersion of 90%. Thermal stability studies indicated an initial sintering of the Pt particles during the first 4 h of heat treatment at 450 °C in an air environment. After that, there was no noticeable change of the particle size during the following heat treatment process. Carbon monoxide oxidation demonstrated nearly 100% conversion of CO to CO₂ over 20 mg of 4.8×10^{-6} mg Pt/cm² loaded silica gel particles at 180 °C for 100 sccm flow rate of 1% CO in argon.

© 2010 Elsevier B.V. All rights reserved.

1. Introduction

Novel mesoporous nanostructured materials which have extremely high surface area and low density have attracted a lot of attention and have been studied extensively for the design of heterogeneous catalysts for the application of catalytic reforming for fuel production, fuel cells, batteries and pollution control etc. [1–4]. There are several benefits associated with a mesoporous substrate for catalyst applications: (1) it has a pore size between 5 and 50 nm, which favors the transport of reagents and/or products within the catalyst structure. Since many catalytic reactions are transport-limited, the use of a mesoporous support may enhance the reaction; (2) the large surface area of the support helps to improve the catalyst efficiency since more metal surface will be exposed to the reaction per mass of metal supported substrate; and (3) the extremely large surface area and tortuous structure of the substrate provide improved stabilization for supported metal particulate catalyst.

Atomic layer deposition (ALD) is a surface controlled chemical reaction process, which is based upon the principle of splitting a binary reaction into two half-reactions and alternating the exposure of gas phase precursors for each half-reaction to a surface

[5]. Due to its self-limiting sequential chemical reaction mechanism, ALD is particularly well suited for uniform deposition of ultra thin films on nanosized particles. Because it is independent of line-of-sight, it allows nanometer scale functionalization within pores as well as on the surface of porous substrates. ALD has been used recently to deposit various materials on porous nanostructures and carbon aerogels [6–13]. For example, King et al. [11] showed that the Pt loading and Pt particle size decreased as the depth of the sample increased for carbon aerogel monoliths. The challenge for this process is that it is very difficult for the precursor to penetrate into nano-sized pores that are deep inside of the sample when the sample is large enough. The catalyst performance can be sensitive to metal particle size because the surface structure and electronic properties can change greatly in the 1–50 nm size range. It is also important for the nanoparticle catalyst to have a relatively narrow particle size distribution. Hence, in order to achieve the maximum benefit from an extremely high surface area substrate, it is desirable to homogeneously disperse the catalyst onto large quantities of particulate substrate materials while maintaining a narrow particle size distribution of the catalyst. The resultant catalyst particles can be further processed to fabricate catalyst for pellets or other configuration specific applications.

Atomic layer deposition carried out in fluidized bed reactors (ALD-FBR) shows great potential to fulfill this objective since it has been used successfully to deposit uniform ceramic, metal and hybrid ceramic/polymer films on large quantities of micron,

* Corresponding author. Tel.: +1 303 492 3759; fax: +1 303 492 4341.

E-mail address: alan.weimer@colorado.edu (A.W. Weimer).

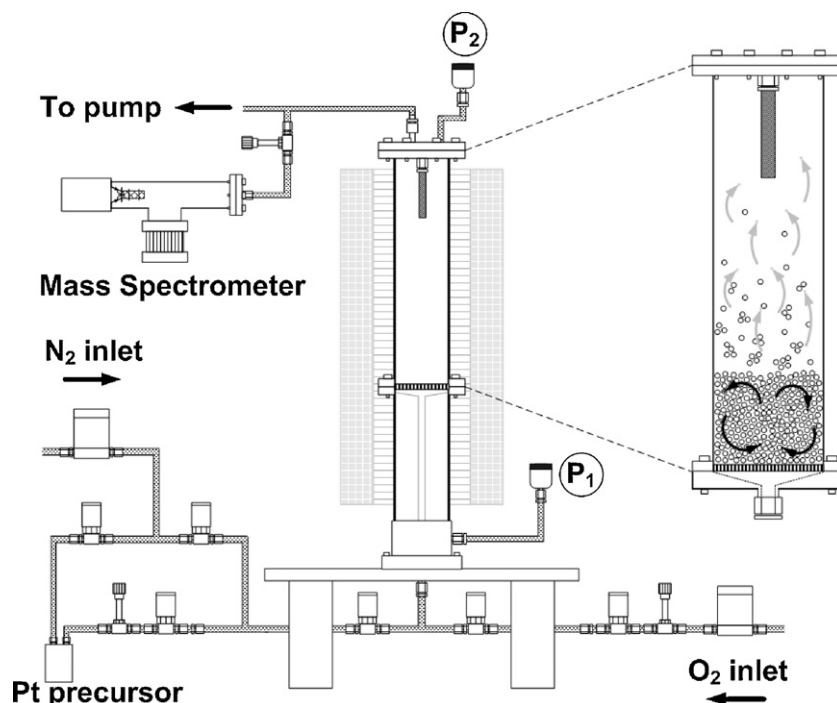


Fig. 1. Schematic of the fluidized bed reactor configuration with *in situ* mass spectrometry for particle ALD.

submicron and nano-sized particles [14,15]. An important feature of using an ALD-FBR for particle coating is its ability to nanocoat individual primary particles instead of aggregates of particles. Aggregates are dynamically broken and reformed allowing exposure to all particle surfaces during coating. The model system for this study is to disperse Pt nanoparticles onto large quantities of mesoporous silica gel particles (8 g). Through this study, it is demonstrated that an ALD-FBR process is an effective method for dispersing nanoparticulate catalysts onto large quantities of mesoporous substrates. The distribution of the catalyst is homogeneous on each primary porous particle substrate and through the entire volume of substrate particles.

2. Experimental

2.1. Supported catalyst preparation by ALD

The fluidized bed reactor (FBR) was designed and constructed for the delivery of reactive gases to functionalize particles at large scale. The process is easily scaled-up. High surface area nano- and micron-sized particles can be effectively fluidized by flowing an inert carrier gas, assisted by mechanical agitation of the powder bed, if needed. A schematic of the system is shown in Fig. 1. The reactor itself was composed of a 3.5 cm inside diameter stainless steel tube with a 10 μm pore size porous metal disc as the gas distributor. The fluidization process provides for inherent contact efficiency between the precursor and particle substrates. This system has been described in detail elsewhere [16,17]. Micron-sized porous silica gel particles, purchased from Aldrich, were used as the catalyst support in this study. The particle size of the silica gel is 30–75 μm , pore volume is 0.75 cm^3/g , pore size is 6 nm, and the surface area is 513 m^2/g .

In order to assure sample powder fluidization during the ALD coating process, the superficial gas velocity was kept above the minimum fluidization velocity (U_{mf}). U_{mf} was determined by measuring the pressure drop across the bed of particles as a function of the delivered N_2 flow rate. The background pressure drop pro-

file was measured without powder in the reactor. This pressure drop was then subtracted from the pressure drop measurement obtained for the reactor with powder. This provides the pressure drop resulting from the powder bed alone, as shown in Fig. 2. The arrow identifies the point of minimum superficial gas flow rate in order to maintain powder fluidization in the reactor. Also, mechanical agitation has been shown to help maintain fluidization behavior more consistently. The flow rate of 0.3 cm/s was used to maintain fluidization for both nitrogen carrier gas and oxygen dosing for the coating process. Eight grams of silica gel substrate were processed in the ALD-FBR. In order to control the ALD process efficiently, an in-line residual gas analyzer (RGA) was placed downstream of the reactor. The RGA is part of a Quadrupole Mass Spectrometer (QMS200 Stanford Research Systems, Sunnyvale, CA). Gas samples out of the ALD-FBR were continuously analyzed by the QMS. The QMS fragments each chemical species that flows through and provides a “fingerprint” of each chemical. QMS detection of the reaction residual gases was used to determine when each half-reaction was completed. In this manner, dose time was easily determined for

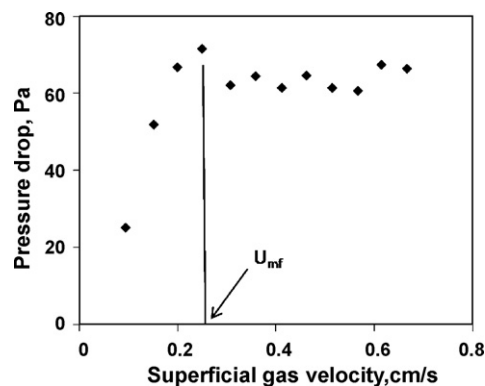


Fig. 2. Pressure drop across the fluidized bed versus superficial gas velocity for 8 g silica gel particles at 325 °C.

a given total surface area of particles and reactant precursor feed rate.

2.2. Characterization

2.2.1. BET surface area

The specific surface area of the substrate and supported catalysts was calculated by the Brunauer–Emmett–Teller (BET) method from the N_2 adsorption isotherms obtained at 77 K. The measurements were carried out using a Micromeritics' Gemini V Series Surface Area Analyzer. Prior to the analysis, the samples were treated at 80 °C for 4 h under vacuum.

2.2.2. ICP

The concentration of Pt on porous silica substrates was analyzed using inductively coupled plasma atomic emission spectrometry (ICP-AES). ICP-AES provides the concentration in parts per million (ppm) by mass of Pt in relation to the porous particles.

2.2.3. Transmission electron microscopy (TEM)

The morphology and Pt particle size distribution (PSD) were investigated using a Philips CM-200 microscope. The cross-sectioned TEM samples were prepared by cutting the epoxy resin cured catalyst particles using a diamond knife. The thickness of the cross-sectioned sample is about 80 nm.

2.2.4. H_2 chemisorption

Hydrogen chemisorption studies were carried out on an Autosorb-1 from Quantachrome Instruments. Prior to the measurement, the samples were evacuated at 350 °C for 60 min followed by H_2 reduction at 350 °C for 4 h. After reduction, the samples were evacuated at 350 °C for 90 min to remove any residual H_2 , and then cooled to 40 °C for analysis. The total H_2 adsorption was obtained in the 1st measurement. After the 1st measurement, the sample was evacuated at the analysis temperature to 10^{-6} Torr and a 2nd measurement was taken. The adsorption obtained in the 2nd measurement is a reversible adsorption. The difference between the 1st and 2nd measurement is the irreversible adsorption (strong chemisorption). In order to determine the average particle size of supported metals from H_2 chemisorption, monolayer coverage (complete surface coverage) of H_2 on metal was used. Metal dispersion is measured as the fraction of metallic atoms present on the surface and therefore determines the catalytic properties. Assuming that the particles are spherical, the equivalent particle diameter (d) was estimated and calculated by the following equation [18]:

$$d = \frac{100 \times L \times f}{ASA \times Z}$$

where L is the mass, Z is the density, ASA is the metal surface area, and f is a particle shape correction factor (=6 for spherical particles).

2.2.5. CO oxidation

The catalytic activity of the Pt-ALD deposited silica gel was characterized in a continuous flow reactor constructed of stainless steel tubing. 20 mg of catalyst particles were sandwiched between two porous stainless steel filters. Gases were preheated by flowing them through a 10 cm long heated tube. The reactor tube was heated using a temperature controlled (Watlow) heat tape. Dry argon, oxygen and carbon monoxide were fed into the system and their flow rates were controlled by mass flow controllers. The concentrations of gases were monitored with an internal QMS (Stanford Research Systems). For every test, the concentration of oxygen, carbon monoxide and carbon dioxide were calibrated before heating the samples to the reaction temperature.

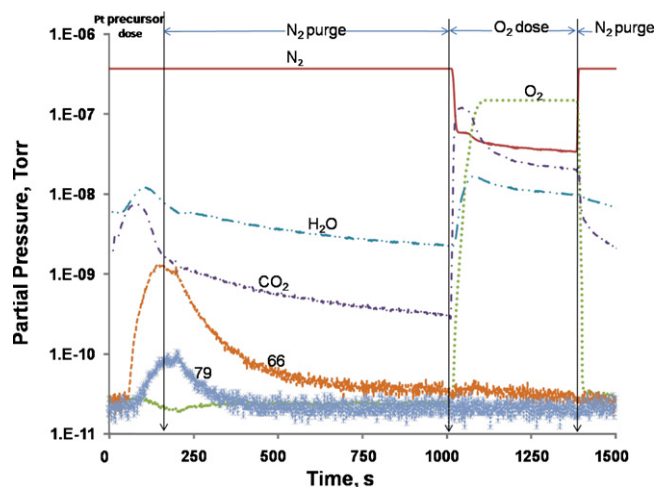


Fig. 3. *In situ* mass spectrometry results during one complete Pt ALD cycle.

3. Results and discussion

3.1. Catalyst preparation

Nanometer sized platinum particles were dispersed onto the mesoporous silica powder substrate using an ALD-FBR. The ALD growth of platinum is from the metal–organic precursor [MeCpPtMe₃: (methylcyclopentadienyl) trimethyl platinum] and oxygen. MeCpPtMe₃ is a solid precursor, which is vaporized at room temperature. An evaporation temperature of 65 °C for the MeCpPtMe₃ yielded a sufficient partial pressure for the ALD reaction. The silica gel substrate temperature was kept at 325 °C throughout the experiment.

The precursor dose and purge times were determined using the on-line mass spectra. A typical curve which can be observed for the ALD process is shown in Fig. 3. Each half-reaction was clearly observed and indicated that the chemistry was self-limiting. When Pt precursor was dosed into the reactor, there was an increase in the partial pressure of water and CO₂. Soon after, the water and CO₂ subsequently decreased, which indicated that the surface was saturated and the reaction had reached completion; the partial pressure of Pt precursor fragment (mass 66 and 79) began to increase, which

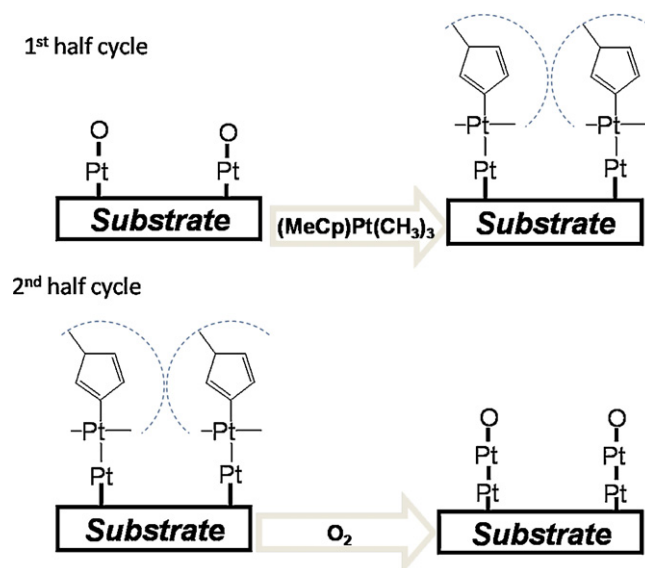


Fig. 4. Pt ALD mechanism.

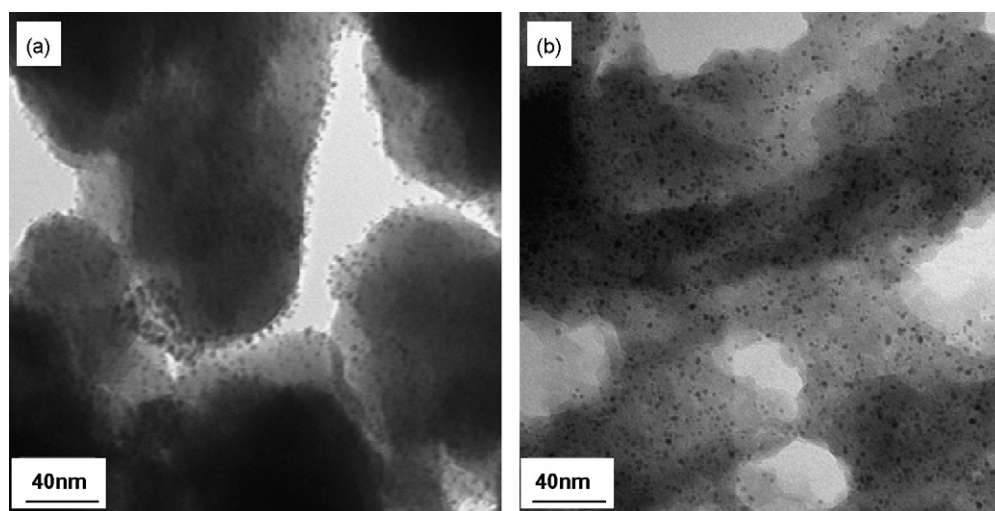


Fig. 5. TEM images of 10 cycles of Pt ALD coated silica gel: (a) plan view and (b) cross-sectioned view.

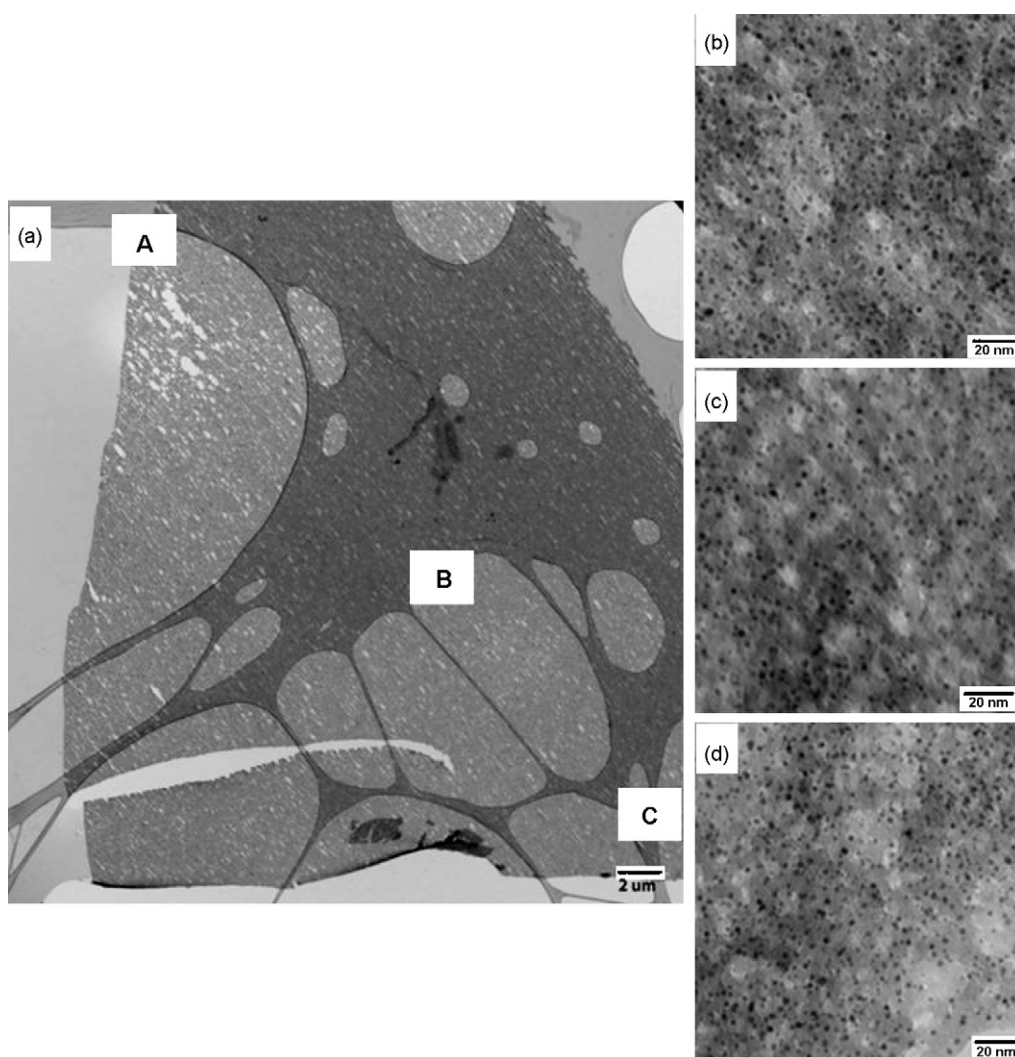


Fig. 6. TEM images of 10 cycles of Pt ALD coated silica gel: (a) low magnification, (b) high magnification at location A, (c) high magnification at location B and (d) high magnification at location C.

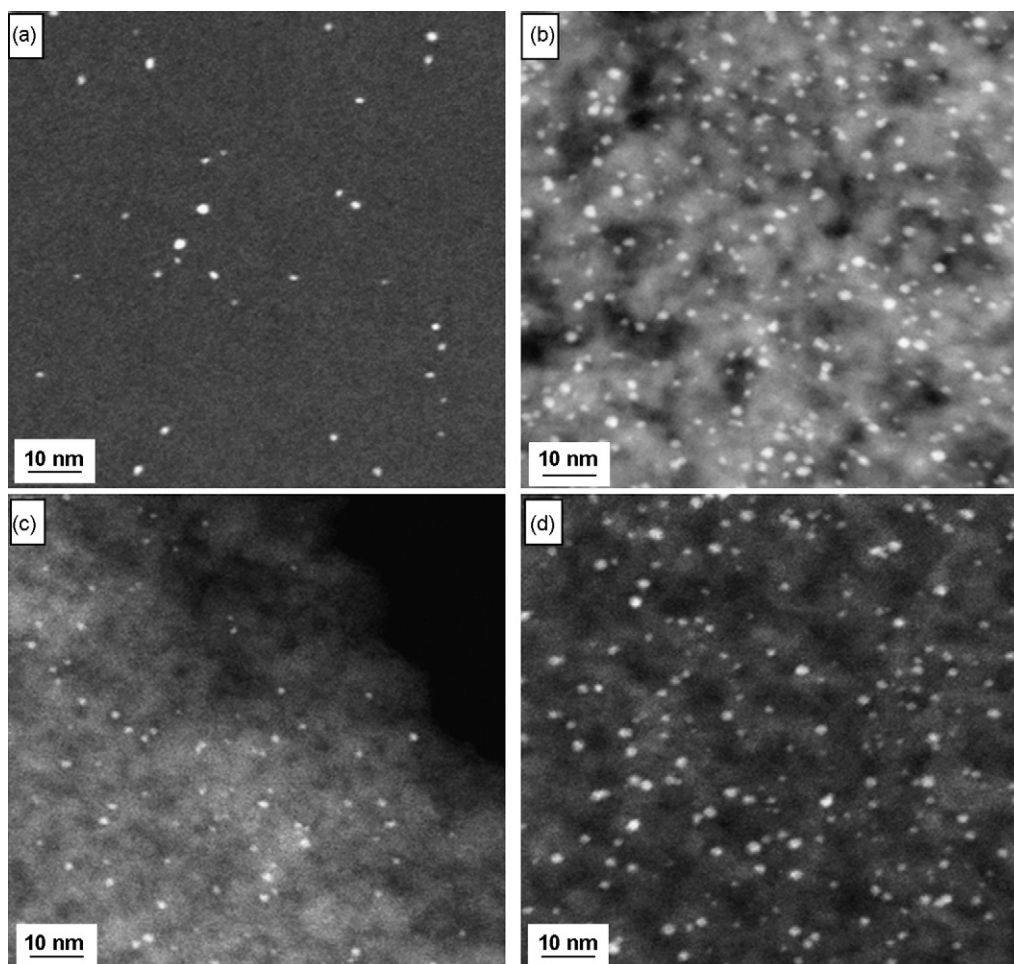
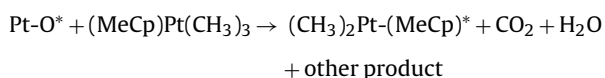


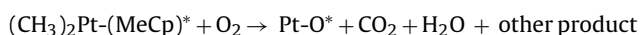
Fig. 7. TEM images of 3 cycles of Pt ALD coated silica gel: (a) as deposited, (b) after 4 h of heat treatment at 450 °C, (c) after 8 h of heat treatment at 450 °C and (d) after 4 h of heat treatment at 750 °C.

signified the precursor breakthrough, and eventually reached a maximum. After the reactor was purged, oxygen was dosed and the partial pressure of water, CO₂ and oxygen increased. As oxygen continued to be dosed, the reaction product concentration began to decrease, which signified that the reaction was approaching completion. The primary molecular mass peaks are 18, 28, 32 and 44 identified for water, nitrogen, oxygen, carbon dioxide; and fragmentation peaks are 66 and 79 from the Pt precursor, respectively. As soon as the Pt precursor fragment is seen (i.e. “breakthrough”), the precursor dosing is terminated. This control strategy minimizes unnecessary precursor waste and provides for efficient use of expensive noble metal catalyst precursors. The process can be optimized for commercial application with essentially no precursor waste. Under identical ALD deposition conditions, Pt was dispersed on the mesoporous silica substrate with 3, 5 and 10 cycles. Based on the observation of mass or fragmentation signals through the on-line mass-spectra, it is proposed that the Pt ALD mechanism using (methylcyclopentadienyl) trimethyl platinum and O₂ as precursor is:

1st half cycle:



2nd half cycle:



where “*” represents an active surface species, and Pt-O* represents oxygen that is adsorbed on the platinum surface [19]. Surface studies have shown that oxygen atomically adsorbs on the platinum surface at room temperature under ultrahigh vacuum (UHV) conditions [20–22]. The schematic diagram showing the reaction that occurs during each half cycle is shown in Fig. 4.

3.2. Catalyst characterization

The BET results show that the specific surface area of the mesoporous silica gel was decreased after Pt nanoparticles were coated within the pores. The surface area for coated silica gel samples after 3 cycles of Pt ALD coating was reduced from 513 m²/g (pure silica gel) to 482 m²/g, and after 10 cycles to 408 m²/g. There are several reasons attributed to the reduction of surface area with an increase in the number of ALD coating cycles. In one aspect the surface area is being reduced as a result of increased particle density due to Pt deposition. Another aspect of the surface area reduction is most likely due to the blocking of micro-pores. According to calculated Pt loadings, the surface area increase from Pt deposition itself is relatively small. ICP results revealed a Pt concentration of 1.6 wt.% for 3 cycles, 2.3 wt.% for 5 cycles and 12 wt.% for 10 cycles, respectively. These results suggest an extremely low Pt loading which is 3.1×10^{-6} mg/cm² (0.10 atom/nm²), 4.8×10^{-6} mg/cm² (0.15 atom/nm²) and 2.9×10^{-5} mg/cm² (0.91 atom/nm²) for 3, 5 and 10 coating cycles, respectively. These values were calculated based on the ICP results and BET surface area measurements. The

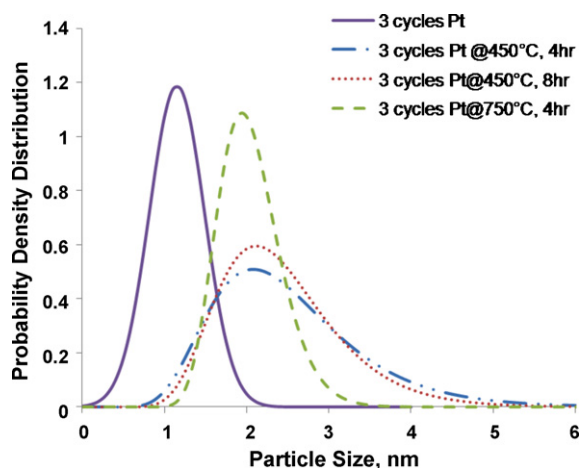


Fig. 8. particle size distribution of as deposited and heat treated 3-cycle Pt-ALD deposited silica gel particles.

lower growth rate for the first 5 coating cycles is attributed to the existence of an ALD incubation period which agrees with King and Altonen's observations [11,23].

Bright field TEM images were taken from the outer surface (Fig. 5a) and a cross-sectioned surface (Fig. 5b) of mesoporous silica gel after 10 cycles of Pt ALD coating. These figures clearly indicate that the Pt particles are homogeneously dispersed on both the outer surface of the porous silica gel substrate and the inside surface of the porous structure. The average Pt particle size is about 2.3 nm with a narrow particle size distribution across the entire inner and outer particle surface.

TEM images were taken from 3 different locations on the sample with 10 cycles of Pt ALD coating as identified in Fig. 6a. The distance between adjacent spots is about 30 μm . As shown in Fig. 6b–d, the density and the size of the Pt particles are similar which confirms the hypothesis that the particles are well dispersed throughout the entire structure for each single silica gel particle. The TEM image from as-deposited 3 cycles ALD coated mesoporous silica gel shows that the Pt particle size is about 1.2 nm. This observation demonstrates that ALD has great capability to disperse catalytic sites onto large quantities of high surface area mesoporous substrates. This result is a significant improvement compared to the results reported in the previous literature [11], in which the average Pt particle size decreased from 4.2 nm to 2.3 nm from the surface to a 10 μm depth within the porous substrate. Uniform and narrow Pt size distribution is important for the catalyst's selectivity performance.

H_2 chemisorption results showed (Table 1) that the irreversible monolayer uptake by H_2 absorption is 37 $\mu\text{mol/g}$ for 3 cycles ALD coated Pt catalyst, and it was 119 $\mu\text{mol/g}$ for 10 cycles of ALD Pt coating. The metal dispersion was decreased from 90% to 46% due to the increased Pt particle size. The surface activity of the sample with 10 cycles of Pt ALD is much higher than that of the 3 cycles coated sample, due to the higher Pt loading after 10 cycles of Pt ALD. However, the higher metal dispersion results in higher catalytic usage efficiency. Based on the H_2 chemisorption measurements, the mean Pt particulate size is ~ 1.3 nm, ~ 2.1 nm and ~ 2.4 nm for 3,

5 and 10 cycles coating, respectively, which is consistent with the average Pt particle sizes observed by TEM. The average particle size measured by the H_2 chemisorption method is based on the entire sample amount used in the experiment which is normally 1 g. The agreement between the chemisorption result and the TEM characterization result provides further evidence that the Pt particle size distribution is uniform through the entire particle.

3.3. Pt thermal stability testing

Sintering of supported catalytically active nanoparticles during chemical reactions at elevated temperatures often leads to the loss of the catalytic activity and the selectivity of the catalyst particles [24–26]. In order to study the thermal stability of the supported Pt catalyst, the samples with 3 cycles of Pt coating were heated to and maintained at 450 $^\circ\text{C}$ for 4 and 8 h in air at atmospheric pressure, respectively. Further testing of the samples for high temperature was heating to 750 $^\circ\text{C}$ and then maintaining the samples at this temperature for 4 h. Scanning transmission electron microscopy (STEM) images taken from the as deposited sample are shown in Fig. 7a. Images taken from the samples that have been heat treated at 450 $^\circ\text{C}$ for 4 and 8 h and heat treated at 750 $^\circ\text{C}$ for 4 h are shown in Fig. 7b–d, respectively. The particle size distributions of the as deposited sample and that after heat treatment are plotted in Fig. 8. The average Pt particle of the as deposited sample is about 1.2 nm. After the heat treatment, the average Pt particle size increased to 2 nm. It is suggested that sintering occurred between the nearby Pt particles during the heat treatment process, which resulted in the formation of larger sized Pt particles. Continuous heating at 450 $^\circ\text{C}$ from 4 h to 8 h showed that there was no significant sintering resulting from the additional heat treatment. This study suggests the possibility that, if a certain distance is maintained between the adjacent particles, then the attractive force between them may be too small to cause additional sintering. As shown in the TEM image of the sample after 4 h of heat treatment at 750 $^\circ\text{C}$, the major part of the sintered Pt particle is still about 2 nm. Clearly, it can be concluded that the Pt nanoparticles were not stable as deposited. They sintered and formed larger particles at elevated temperatures.

3.4. CO oxidation

The catalytic activity of the 5-cycle Pt-ALD deposited silica gel was evaluated by CO oxidation, as shown in Fig. 9. First, the CO oxidation reaction was studied as a function of the reaction temperature. The total flow rate of the gas is 100 sccm over 20 mg of catalyst. The N_2/O_2 ratio is 80/20 vol.% and the CO/O_2 molar ratio is kept at 0.05, which is about 1% CO in total. 99% conversion of CO to CO_2 was observed when the reaction temperature of 180 $^\circ\text{C}$ was applied. The conversion vs. the gas flow rate was also studied. As the gas flow rate increased, the conversion rate decreased, as shown in Fig. 9b.

The turnover frequency (TOF) of the Pt-Silica catalyst was estimated based on ICP, chemisorption and CO oxidation results. Our calculation is based on the assumptions that: (1) every surface atom is catalytically active and (2) there is full penetration of reactants throughout the cross-section of the Pt-silica catalyst. For the sam-

Table 1
Summary of characterization result.

Sample description	Pt loading (wt.%)	Particles size (nm)		Dispersion (%)	Monolayer uptake ($\mu\text{mol/g}$)
		TEM	Chemisorption		
3 cycles	1.6	1.2 ± 0.3	1.3	90	37
5 cycles	2.3	1.9 ± 0.2	2.1	53	30
10 cycles	12	2.3 ± 0.2	2.4	46	119

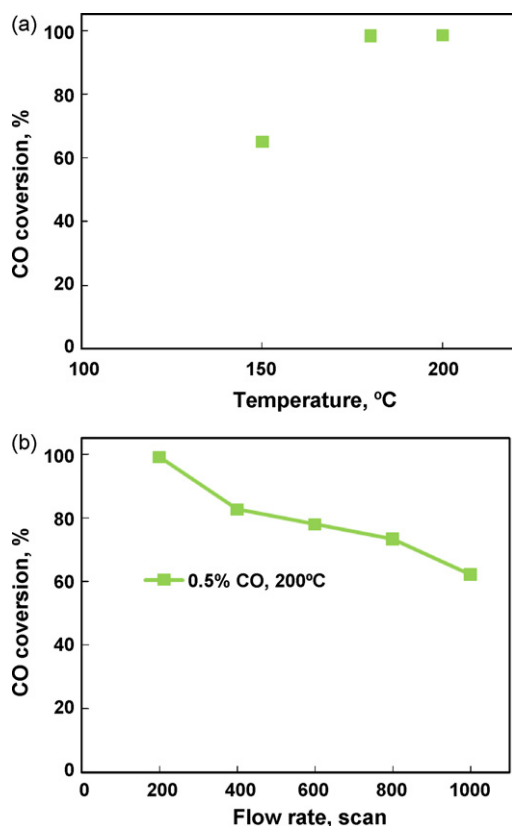


Fig. 9. CO oxidation reaction results for 5 cycle Pt ALD sample (20 mg sample): (a) CO conversion versus temperature with total gas flow rate of 100 sccm and molar CO/O₂ ratio of 0.05 (1% CO in the gas stream) and (b) CO conversion versus gas flow rate with molar CO/O₂ ratio of 0.5 (0.5% CO in the gas stream).

ple with 5 cycles of Pt ALD, this leads to a TOF of 1.8 s^{-1} at the gas flow rate of 1000 sccm and the reaction temperature of 200 °C.

4. Conclusion

In summary, it has been demonstrated that Pt nanoparticles can be homogeneously dispersed onto primary 30–75 μm mesoporous substrate particles using a fluidized bed reactor to carry out particle ALD (i.e. ALD-FBR). The size distribution of the Pt nanoparticles was uniform and narrow across the entire substrate surface. For the mesoporous substrate with 3 cycles of Pt ALD coating, the resulting Pt particle size is 1.2 nm. Under these processing conditions, the

metal dispersion reached 90% providing for efficient use of Pt. Thermal stability studies indicated that there was an initial sintering of the nearby Pt particles. The Pt nanoparticles inside the mesoporous structure were still very small, only ~2 nm after heat treatments at both 450 °C and 750 °C for 4 h. The oxidation reaction of CO demonstrated that for $4.8 \times 10^{-6} \text{ mg Pt/cm}^2$ loading catalyst, nearly 100% conversion of CO to CO₂ was observed at 180 °C with 100 sccm flow rate (1% CO in the stream) over 20 mg of catalyst. This study shows that the ALD-FBR is a promising process option for synthesizing ultra-low loadings of precious metal catalytic sites.

References

- [1] J.B. Joo, P. Kim, W. Kim, J. Yi, *J. Electroceram.* 17 (2006) 713–718.
- [2] D.J. Kim, B.C. Dunn, F. Huggins, G.P. Huffman, M. Kang, J.E. Yie, E.M. Eyring, *Energy Fuel* 20 (2006) 2608–2611.
- [3] B.C. Dunn, D.J. Covington, P. Cole, R.J. Pugmire, H.L.C. Meuzelaar, R.D. Ernst, E.C. Heider, E.M. Eyring, *Chem. Rev.* 18 (2004) 1519–1521.
- [4] Y. Zhang, C.Y. Zhao, H. Liang, Y. Liu, *Catal. Lett.* 127 (2009) 339–347.
- [5] S. George, A. Ott, J. Klaus, *J. Phys. Chem.* 100 (1996) 13121–13131.
- [6] X.H. Liang, S.M. George, A.W. Weimer, *Chem. Mater.* 19 (2007) 5388–5394.
- [7] S. Kucheyev, J. Biener, Y. Wang, T. Baumann, K. Wu, T. van Buuren, A. Hamza, J. Satcher, J. Elam, M. Pellin, *Appl. Phys. Lett.* 86 (2005) 083108.
- [8] J. Biener, T. Baumann, Y. Wang, E. Nelson, S. Kucheyev, A. Hamza, M. Kemell, M. Ritala, M. Leskela, *Nanotechnology* 18 (2007) 055303.
- [9] S. Kucheyev, J. Biener, T. Baumann, Y. Wang, A. Hamza, Z. Li, D. Lee, R. Gordon, *Langmuir* 24 (2008) 943–948.
- [10] J. Elam, J. Libera, M. Pellin, A. Zinovev, J. Greene, J. Nolen, *Appl. Phys. Lett.* 89 (2006) 053124.
- [11] J. King, A. Wittstock, J. Biener, S. Kucheyev, Y. Wang, T. Baumann, S. Giri, A. Hamza, M. Baeumer, S. Bent, *Nano Lett.* 8 (2008) 2405–2409.
- [12] E.L. Lakomaa, *Appl. Surf. Sci.* 75 (1994) 185–196.
- [13] E.L. Lakomaa, S. Haukka, T. Suntola, *Appl. Surf. Sci.* 60–61 (1992) 742–748.
- [14] X.H. Liang, D.M. David, P. Li, S.M. George, A.W. Weimer, *AIChE J.* 55 (2009) 1030–1038.
- [15] L. Hakim, D. King, Y. Zhou, C. Gump, S. George, A. Weimer, *Adv. Funct. Mater.* 17 (2007) 3175–3181.
- [16] D. King, J. Spencer, X. Liang, L. Hakim, A. Weimer, *Surf. Coat. Technol.* 201 (2007) 9163–9171.
- [17] X.H. Liang, L.F. Hakim, G.D. Zhan, J.A. McCormick, S.M. George, A.W. Weimer, J.A. Spencer, K.J. Buechler, J. Blackson, C.J. Wood, J.R. Dorgan, *J. Am. Ceram. Soc.* 90 (2007) 57–63.
- [18] Quantachrome Instruments Autosorb 1C Chemisorption Operational Manual, 2007.
- [19] M. Hiratani, T. Nabatame, Y. Matsui, K. Imagawa, S. Kimura, *J. Electrochem. Soc.* 148 (2001) C524–C527.
- [20] T. Matsushima, D.B. Almy, J.M. White, *Surf. Sci.* 67 (1977) 89–108.
- [21] J.L. Gland, B.A. Sexton, G.B. Fisher, *Surf. Sci.* 95 (1980) 587–602.
- [22] C.T. Campbell, G. Ertl, H. Kuipers, J. Segner, *Surf. Sci.* 107 (1981) 220–236.
- [23] T. Aaltonen, M. Ritala, T. Sajavaara, J. Keinonen, M. Leskela, *Chem. Mater.* 15 (2003) 1924–1928.
- [24] B. Min, A. Santra, D. Goodman, *Catal. Today* 85 (2003) 113–124.
- [25] K. Hayashi, T. Horiuchi, K. Suzuki, T. Mori, *Catal. Lett.* 78 (2002) 43–47.
- [26] Z. Chen, G. Smith, C. Putman, E. ter Voert, *Catal. Lett.* 50 (1998) 49–57.